CHARACTERIZATION OF $(H_2O)_n^-$ CLUSTERS USING MODEL POTENTIAL APPROACHES

by

Xiaoge Su

B.S. in Chemical Physics,

University of Science and Technlogy of China, 2008

Submitted to the Graduate Faculty of

the Kenneth P. Dietrich School of Arts and Sciences in partial fulfillment

of the requirements for the degree of

Master of Science

University of Pittsburgh

2013

UNIVERSITY OF PITTSBURGH

DEPARTMENT OF CHEMISTRY DIETRICH SCHOOL OF ARTS AND SCIENCES

This was presented

by

Xiaoge Su

It was defended on

November 5, 2013

and approved by

K.D. Jordan, Ph.D., Professor

R.D. Coalson, Ph.D., Professor

G.R. Hutchison, Ph.D., Professor

Committee Chair: K.D. Jordan, Ph.D., Professor

CHARACTERIZATION OF $(H_2O)_n^-$ CLUSTERS USING MODEL POTENTIAL APPROACHES

Xiaoge Su, M.S.

University of Pittsburgh, 2013

$(H_2O)_n^-$ clusters have attracted considerable interest since their discovery. Experimentally, three kinds of isomers of $(H_2O)_n^-$ have been identified, but the relationship between the cluster size and the distribution of the excess electron is unknown. The pathways for conversion of the surface- to cavity-bound electron are also controversial. In this thesis, molecular dynamics simulations are applied using a $(H_2O)_n^-$ model introduced by the Jordan group. It is found that for $(H_2O)_6^-$, the tweezers structure rapidly evolves to the more stable AA structure, however for book structure the energy barrier is much higher and formation of the AA isomer is not observed on the picosecond time scale.

TABLE OF CONTENTS

LIST OF TABLES

LIST OF FIGURES

Acknowledgements

First and foremost I would like to thank my advisor Dr. Kenneth D. Jordan for the continuous support of my master study and research, for his patience, motivation, enthusiasm and immense knowledge.

I also wish to thank past and current labmates in the Jordan group: Jiawei Xu, Guozhen Zhang, Jing Ding, Tae-hoon Choi, Ozan Karalti, Sefa Karalti, Eric Kratz, Fangfang Wang, Aude Marjolin, Zach Pozun, Meysam Makaremi, Michael Deible, Xun Wang, Anshuman Thakur, Togo Shmogo and Kaye Archer, for all the fun we have had in the last four years.

Finally, I would like to dedicate this thesis to Mizuki Nana.

1.0 INTRODUCTION

The hydrated electron, e_{aq}^-, has attracted considerable attention since its discovery in 1962.[1] e_{aq}^- is involved in a wide range of processes, including the generation of hydrogen gas in water-cooled nuclear reactors, corrosion reactions, breaking of DNA strands, and many catalytic reactions, including those involved in the induced destruction of organic wastes.[2] Because of the challenges of studying e_{aq}^- many groups have turned to $(\mathrm{H_2O})_n^-$ clusters that can be more readily characterized by experiment and theory.

Electronic absorption, photoelectron spectroscopy,[3] and vibrational spectroscopy[4] have identified three different kinds of isomers of $(\mathrm{H_2O})_n^-$ clusters designated **I**, **II** and **III**. Isomer **I** has been interpreted as binding the excess electron in the interior; while isomers **II** and **III**, have been interpreted as binding it at the surface.[5] The vertical electron detachment energy (VDE) of isomer **I** is higher than that of the other two isomers, and its dependence on the size of the cluster is also much stronger.[6] Experiments have shown the photodetachment energy of isomer **I** converges to that of e_{aq}^- with increasing size, as does the electronic absorption

1

spectrum. The relaxation times of the electronically excited states of isomers **II** and **III** are much longer than for isomer **I**.[6]

The cluster size where the internal state becomes energetically more favorable is controversial, with estimates ranging from $n = 14$ to 200.[7,8] Also, the pathways for conversion of the surface- to cavity-bound electron are unknown. For small clusters the electron is bound by the dipole field, while correlation effects tend to dominate for large clusters.[9] In the experiments,[5] the temperature of the clusters is usually under 100K; which means they are solid-like and probably "freeze in" the initial structures.[10] Surface-bound excess electron states for the clusters are also relevant to understanding the nature of an excess electron at the interface of bulk water.[11]

Commonly used ab-*initio* methods are either not adequate or are too computationally demanding for studies of the pathways and for simulations of the dynamics of the anions, especially for large clusters. Recently, density-functional theory (DFT) has been applied to this problem.[9,10,12,13] However DFT suffers from self-interaction error and the failure to describe dispersion interactions. The most viable approach for theoretical studies of $(H_2O)_n^-$ clusters is to make use of one-electron model Hamiltonians.[14] Ab-*initio* calculations carried out in the Jordan group show that the models used in recent studies[15–17] have sizable errors due to deficiencies in both the water model and the one-electron Hamiltonian.

In order to simulate the properties of $(H_2O)_n^-$ clusters, it is essential to combine a reliable one-electron Hamiltonian and a neutral water force field with an efficient molecular dynamics code. This has been a major goal of my research to date. Longer range goals include using this software to map out the pathways between surface-bound and cavity-bound excess electron states, and to extend the studies to the excess electron in bulk water.

2.0 THEORETICAL BACKGROUND

2.1 FORCE FIELD OF NEGATIVELY CHARGED WATER CLUSTERS

2.1.1 Distributed point polarizable water model

The distributed point polarizable model, aka. DPP (Figure. 1) is first described. It is a

rigid water model with four terms:[14]

1. Electrostatics is represented in terms of permanent charges located at the hydrogens and

   at an M site. The resulting charge-charge intermolecular interactions are

$$E_{coulomb} = \sum_{i,j} \frac{q_i \cdot q_j}{r_{ij}}.$$

(2.1)

2. Polarization is described by mean of point inducible dipole, and each atom is polarizable

   and mutually interacting with the polarizable sites on other atoms. The polarization
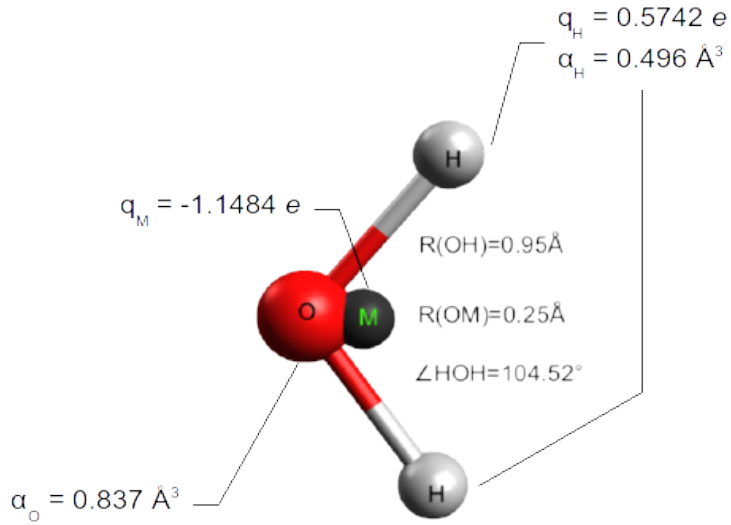
Figure 1: DPP water model

energy is given by

$$E_{pol} = -0.5 \sum_i \vec{E}_i \cdot \vec{\mu}_i, \qquad (2.2)$$

where $\vec{E}_i$ is the electric field at atom i and $\vec{\mu}_i$ is the dipole of atom i, given by

$$\vec{\mu}_i = \alpha_i \left[\vec{E}_i + \sum_{i \neq j} \overleftrightarrow{T}_{ij} \cdot \vec{\mu}_j \right]. \qquad (2.3)$$

Here α_i is the isotropic polarizability for atom i and $\overleftrightarrow{T}_{ij}$ is the dipole tensor with elements

5

defined by

$$T_{ij}^{\beta\gamma} = f_5(r_{ij})\frac{3r_{ij}^{\beta}r_{ij}^{\gamma}}{r_{ij}^5} - f_3(r_{ij})\frac{\delta_{\beta\gamma}}{r_{ij}^3}, \tag{2.4}$$

and the electric field is given by

$$\vec{E}_i = \sum_{j \neq i} f_3(r_{ij})\frac{q_j(r_{ij})\vec{r}_{ij}}{r_{ij}^3}. \tag{2.5}$$

In (2.4) and (2.5), f_3 and f_5 are damping functions from Thole,[18] of the form

$$f_3(r_{ij}) = 1 - \exp\left(-a\frac{r_{ij}^3}{\sqrt{\alpha_i\alpha_j}}\right) \tag{2.6}$$

$$f_5(r_{ij}) = 1 - \left(1 + a\frac{r_{ij}^3}{\sqrt{\alpha_i\alpha_j}}\right)\exp\left(-a\frac{r_{ij}^3}{\sqrt{\alpha_i\alpha_j}}\right). \tag{2.7}$$

Here different a values are used in electric field and dipole damping.

3. Dispersion interactions are included between O atoms only, using

$$E_{disp} = \sum_{i,j \to \mathbf{O}} f_6(r_{ij})\frac{C_6}{r_{ij}^6}, \tag{2.8}$$

where $f_6(r_{ij})$ is the Tang-Toennies damping function[19] with $n = 3$. The general form of

the Tang-Tonnies founction is:

$$f_{2n}(R) = 1 - \left(\sum_{k=0}^{2n}\frac{(cR)^k}{k!}\right)\exp\left(-cR\right), \tag{2.9}$$

6

where c is a coefficient that controls the damping.

4. Repulsion between atoms of different monomers is accounted for by a sum of exponential terms:

$$E_{rep} = \sum_{i,j} A_{i,j} \exp(-b_{ij} r_{ij}) \tag{2.10}$$

The values of parameters in the various terms are given in Table 1. The charges on hydrogen atoms and the M site are taken from the TTM2-R model;[20] while the polarization damping factors are fit to the results of MP2/aug-cc-pVTZ[21] calculations.

2.1.2 One-electron polarizable model (OEPM)

To describe the binding of an excess electron to water clusters, a polarization model has been developed.[22,23] In this model the Hamiltonian for the excess electron is

$$\boldsymbol{H} = -\frac{1}{2}\nabla^2 - \sum_i \frac{Q_i}{r_i} f_{pc}(r_i) + \sum_i V_i^{rep} +$$
$$\sum_i \frac{\vec{\mu}_i \cdot \vec{r}_i}{r_i^3} f_{ind}(r_i) - \sum_i \frac{\alpha}{2r_i^4} f_{pol}(r_i). \tag{2.11}$$

The first term is the kinetic energy operator. The second and fourth terms are due to the interaction of the electron with the charges and the induced dipoles of the DPP model. The third term is the short-ranged repulsive potential, which accounts for orthogonality.

7

Table 1: DPP Parameters

Charges	(elem. charge)	Polarizability	(Å^3)
q_H	0.5742	α_H	0.496
q_M	-1.1484	α_O	0.837
Repulsion A	(kcal/mol)	Repulsion B	(Å^{-1})
A_{O-O}	1.15272×10^5	B_{O-O}	4.1679
A_{O-H}	1.80366×10^3	B_{O-H}	3.5355
A_{H-H}	1.19085×10^5	B_{H-H}	5.5817
Dispersion C	(Å^6kcal/mol)	Dispersion c	(kcal/mol)
	-1300		2.23
Charge-dipole damping a	0.23	Dipole-dipole damping a	0.3

The last term involves the polarization of the water by the excess electron. α is the polarizability of a water molecule, which has been found experimentally to be 1.45 Å^3. $f_{pol}(r_j) = (1 - \exp(-br_j^3))^2$ damps the potential to remove divergence when $r_j \to 0$. To reduce the computational complexity, the dipoles on the atoms were collapsed to the M site.

Recently our group has introduced a new self-consistent electron-water polarization model.[24] In the new model, the Hamiltonian is modified to be

$$
\boldsymbol{H} = -\frac{1}{2}\nabla^2 - \sum_i \frac{Q_i}{r_i} f_{pc}(r_i) + \sum_i V_i^{rep}(r_i)
$$

$$
- \frac{1}{2}\sum_{ij}\left[V_{ij}^{e-w,pol}(r_{ie}, r_{ij}) - V_{ij}^{w-w,pol}(r_{ij}) \right], \tag{2.12}
$$

where the term $V_{ij}^{e-w,pol}$ represents both new water-electron and water-water interaction. $V_{ij}^{w-w,pol}$ is the water-water interaction term and comes from the DPP model.

In the self-consistent model, the three polarizable sites of a water molecule are all considered, i.e., not collapsed to one site, in contrast to the model mentioned above. The $\frac{1}{2}V_{ij}^{e-w,pol}$ is expanded to

$$
\frac{1}{2}V_{ij}^{e-w,pol} = \frac{1}{2}\sum_{ij}\left[\vec{E}_i^e(r_ie) + \vec{E}_i^w(r_i) \right] \cdot \left[\alpha_{ii}^{-1} - \overset{\leftrightarrow}{T}_{ij}(r_{ij}) \right]^{-1} \cdot
$$

$$
\left[\vec{E}_j^e(r_je) + \vec{E}_j^w(r_j) \right], \tag{2.13}
$$

where $\vec{E}_i^w$ and $\vec{E}_i^e$ is the static electric field at site i due to the charge sites of the other water

molecules and the excess electron, respectively. α is the site polarizabilities matrix and $\overset{\leftrightarrow}{T}_{ij}$

is the interaction matrix between induced dipoles on sites i and j. To avoid the divergence at

short-range electron-water interaction calculation, r_{ie} is replaced by $d\left[\frac{1}{2} + \left(\frac{r_{ie}}{d}\right)^3 \left(1 - \frac{r_{ie}}{2d}\right)\right]$

when $r_{ie} < d$, where d is the switching parameter. The electric fields on each polarizable

sites are calculated iteratively until convergenced, similar to the DPP model, making the

model self-consistent.

The new model more accurately describes the interaction between the water cluster and

the excess electron, and is used in the simulations in this thesis.

2.1.2.1   Discrete variable approximation

To solve the excess-electron Schrödinger equation, the discrete variable representation

(DVR) method[25,26] was adopted. The conceptual idea of the DVR method is to break the

continuous infinite Hilbert space $\mathcal{H}$ into a discrete finite DVR space $\mathcal{D}$, constituted by fixed

points set $\{x_1, x_2, x_3, ...x_n\}$; then, specially designed functions $|\Delta_i\rangle$, which have the properties

of first-order derivable in $\mathcal{H}$ and $|\Delta_i(x_j)\rangle = \lambda_i \delta_{ij}$, are chosen as a basis set, with the number

of basis functions equal to the number of DVR points.

The DVR space has the following advantage when calculating the matrix elements of the

Hamiltonian $\mathbf{H} = \mathbf{T} + \mathbf{V}$:

$$T_{ij} = \langle \Delta_i | \boldsymbol{T} | \Delta_j \rangle \tag{2.14}$$

which is calculated only once during all the calculations, and

$$V_{ij} = \langle \Delta_i | \boldsymbol{V} | \Delta_j \rangle$$

$$\approx V_i \delta_{ij} \tag{2.15}$$

which implies only diagonal elements in $\mathbf{V}$ need to be calculated.[27] This is the basic approximation of the DVR method, which greatly reduces the cost of matrix element calculation. The solution of the original Schrödinger equation in $\mathcal{H}$ can be approximated by the corresponding Schrödinger equation in DVR space $\mathcal{D}$. The self-consistent field (SCF) iterative method can be used, and it is shown the error is small.[25]

One of the obstacles of using the DVR approach is that in three-dimensional space suitable basis sets $|\Delta\rangle$ are hard to determine, due to the DVR conditions are rather restrictive and cannot be satisfied except on special subspaces of the Hilbert space of wavefunctions.[28] To overcome this difficulty, the basis $|\Delta\rangle$ set is fitted by other basis sets $|\varphi\rangle$, such as sine functions,[28] Bessel functions, or tetrahedral invariant basis.[29] In our implementation, sine

functions are used[22]:

$$\varphi_{ijk}(\vec{x}) = \begin{cases} \displaystyle\prod_{u \in \{i,j,k\}} \sqrt{\frac{2}{L^u}} \sin\left(\frac{i\pi(x^u - x_0^u)}{L^u}\right) & x_0^u \leq x^u \leq x_{n+1}^u \\ \\ 0 & \text{otherwise} \end{cases} \tag{2.16}$$

where $u \in \{i, j, k\}$ indicate the three axis, x_0^u and x_{n+1}^u refer to the box edges, and $L^u = x_{n+1}^u - x_0^u$. The DVR points are distributed in equal spaced grids to ensure $\langle \varphi_{ijk} | \varphi_{uvw} \rangle = \delta_{iu}\delta_{jv}\delta_{kw}$.

2.2 MOLECULAR DYNAMICS

Molecular dynamics (MD) simulations are used to simulate the time-related behavior of the system. During the simulation, each particle follows the Hamiltonian equation:[30]

$$\dot{q}_i = \frac{\partial \mathcal{H}}{\partial p_i}$$
$$\dot{p}_i = -\frac{\partial \mathcal{H}}{\partial q_i} \tag{2.17}$$

where i is the i-th particle in the system, q_i is the position and p_i is the momentum of the particle. $\mathcal{H}$ is the Hamiltonian of the whole system.

The set of all possible $(p_1, ...p_n, q_1, ...q_n)$ points defines the *phase space*.[31] Molecular dy-

namics then simulates the evolution of a phase point inside the defined phase space.[32]

The Liouville operator describes the movement of the phase point:[31]

$$\imath La = \{a, \mathcal{H}\} \tag{2.18}$$

where a is an arbitrary physical variable, $\{\}$ is the Poisson bracket:

$$\{a, b\} = \sum_i \left[\frac{\partial a}{\partial q_i} \cdot \frac{\partial b}{\partial p_i} - \frac{\partial a}{\partial p_i} \cdot \frac{\partial b}{\partial q_i} \right]. \tag{2.19}$$

The evolution of phase point a can be shown to be:[32]

$$\frac{\mathrm{d}a}{\mathrm{d}t} = \imath La$$

$$a(t_0 + \delta t) = \mathbf{e}^{\imath L \delta t} a(t_0) \tag{2.20}$$

When a is the coordinate of phase point, $\mathbf{e}^{\imath L \Delta t}$ defines the time evolution operator of a from t_0 to $t_0 + \delta t$.

2.2.1 Velocity-Verlet integrator

Due to the discrete nature of computer mathematics, the continuous flow of the time has to be divided into discrete time steps. Each time step must be small enough, i.e., 1 fs, to

reduce numerical errors. Denoting the time step as Δt, $a(t_0 + \delta t)$ is split to

$$a(t_0 + \delta t) = \mathbf{e}^{\imath L \delta t} a(t_0)$$

$$= \underbrace{\mathbf{e}^{\imath L \Delta t} \times \mathbf{e}^{\imath L \Delta t} \ldots \times \mathbf{e}^{\imath L \Delta t}}_{\text{total } \delta t / \Delta t \text{ terms}} a(t_0). \tag{2.21}$$

Each $\mathbf{e}^{\imath L \Delta t}$ term is expanded to

$$\mathbf{e}^{\imath L \Delta t} = \mathbf{e}^{\Delta t \times \left(a \frac{\partial}{\partial p} + v \cdot \frac{\partial}{\partial q} \right)}, \tag{2.22}$$

where $a = \dfrac{\dot{p}}{m}$ and $v = \dot{q}$, respectively. To further simplify this, the Trotter theorem is introduced:[33]

$$\mathbf{e}^{\Delta t \times \left(a \frac{\partial}{\partial p} + v \cdot \frac{\partial}{\partial q} \right)} = \mathbf{e}^{\frac{\Delta t}{2} \times a \frac{\partial}{\partial p}} \mathbf{e}^{\Delta t \times v \cdot \frac{\partial}{\partial q}} \mathbf{e}^{\frac{\Delta t}{2} \times a \frac{\partial}{\partial p}} + \mathcal{O}(\Delta t^3) \tag{2.23}$$

Further expanding the exponents using Taylor series, the Velocity-Verlet algorithm is achieved:[34]

$$p_i(t + \frac{\Delta t}{2}) = p_i(t) + \frac{\Delta t}{2} m_i a(t)$$

$$q_i(t + \Delta t) = q_i(t) + \frac{p_i(t + \frac{\Delta t}{2})}{m_i} \Delta t$$

$$p_i(t + \Delta t) = p_i(t + \Delta t/2) + \frac{\Delta t}{2} m_i a(t + \Delta t). \tag{2.24}$$

The error for Velocity-Verlet algorithm is of $\mathcal{O}(\Delta t^2)$, one order higher than the error

14

due to the Trotter separation. It is also a symplectic integrator,[35] with the result that the Hamiltonian of the system is conserved under a slight perturbation. This implies that applying the integrator alone on a system containing particles without constraints will lead to a simulation in the microcanonical ensemble.

Other algorithms, like the Beeman algorithm[36]$(\mathcal{O}(\Delta t^3))$, are also possible.

2.2.2 NO-SQUISH integrator for rigid bodies

The Velocity-Verlet algorithm does not preserve the rigid body structures during the integration. When rigid bodies are used to reduce the complexity of the system to be simulated, other integrators have to be introduced. Among them, Rattle[37] is perhaps the most widely used one, and can be applied on a whole rigid body or to selected bonds. However, it is only symplectic when the number of iterations goes to infinity.[38] The NO-SQUISH[39] algorithm is a symplectic integrator for rigid bodies, which can be formulated naturally via use of a rotational Hamiltonian and the Trotter theorem.

Unlike Rattle, NO-SQUISH does not include any corrections to velocities. Instead, it splits the movement of the rigid bodies into transitional and rotational parts. The transitional part is directly treated by applying Velocity-Verlet on the center-of-mass of the body; meanwhile the rotational part is done using quaternions.

To represent the Euler rotation matrix using quaternions, the unit quaternion, $\mathbf{q} = \{q_0, q_1, q_2, q_3\}$ with $\sum_i q_i = 1$ is introduced. The rotation matrix from lab coordinate to body-fixed coordinate is then given as:

$$\mathbf{A}(\mathbf{q}) = \begin{pmatrix} q_0^2 + q_1^2 - q_2^2 - q_3^2 & 2(q_1 q_2 + q_0 q_3) & 2(q_1 q_3 - q_0 q_2) \\ \\ 2(q_1 q_2 - q_0 q_3) & q_0^2 - q_1^2 + q_2^2 - q_3^2 & 2(q_2 q_3 + q_0 q_1) \\ \\ 2(q_1 q_3 + q_0 q_2) & 2(q_2 q_3 - q_0 q_1) & q_0^2 - q_1^2 - q_2^2 + q_3^2 \end{pmatrix}. \tag{2.25}$$

The relationships between $\mathbf{q}$ and three Euler angles, θ, ϕ and ψ are:

$$\begin{aligned} q_0 &= \cos\left(\frac{\theta}{2}\right)\cos\left(\frac{\phi + \psi}{2}\right), \quad q_1 = \sin\left(\frac{\theta}{2}\right)\cos\left(\frac{\phi - \psi}{2}\right), \\ q_2 &= \sin\left(\frac{\theta}{2}\right)\sin\left(\frac{\phi - \psi}{2}\right), \quad q_3 = \cos\left(\frac{\theta}{2}\right)\sin\left(\frac{\phi + \psi}{2}\right). \end{aligned} \tag{2.26}$$

The equations of motion can then be written as,[40]

$$\begin{aligned} \dot{\mathbf{q}} &= \frac{1}{2}\mathbf{S}(\mathbf{q})\omega^{(4)}, \\ \dot{\omega}_x &= \frac{\tau_x}{I_{xx}} + \frac{I_{yy} - I_{zz}}{I_{xx}}\omega_y \omega_z, \\ \dot{\omega}_y &= \frac{\tau_x}{I_{yy}} + \frac{I_{zz} - I_{xx}}{I_{yy}}\omega_x \omega_z, \\ \dot{\omega}_z &= \frac{\tau_x}{I_{zz}} + \frac{I_{xx} - I_{yy}}{I_{zz}}\omega_x \omega_y, \end{aligned} \tag{2.27}$$

where $\omega^{(4)} = \{0, \omega_x, \omega_y, \omega_z\}$,

$$\mathbf{S(q)} = \begin{pmatrix} q_0 & -q_1 & -q_2 & -q_3 \\ q_1 & q_0 & -q_3 & q_2 \\ q_2 & q_3 & q_0 & -q_1 \\ q_3 & -q_2 & q_1 & q_0 \end{pmatrix}, \tag{2.28}$$

and τ are the torques in the body-fixed frame and I_{xx}, I_{yy}, and I_{zz} are the diagonalized elements of inertia tensor.

The angular momenta are defined as

$$\mathbf{p} = 2 \begin{pmatrix} -q_1 \omega_x I_{xx} - q_2 \omega_y I_{yy} - q_3 \omega_z I_{zz} \\ q_0 \omega_x I_{xx} - q_3 \omega_y I_{yy} + q_2 \omega_z I_{zz} \\ q_3 \omega_x I_{xx} + q_0 \omega_y I_{yy} - q_1 \omega_z I_{zz} \\ -q_2 \omega_x I_{xx} + q_1 \omega_y I_{yy} + q_0 \omega_z I_{zz} \end{pmatrix}. \tag{2.29}$$

The corresponding rotation Hamiltonian can then be decomposed into three parts:

$$\mathbf{H(p, q)} = \sum_k^{x,y,z} h_k(\mathbf{p, q}) + V(\mathbf{q}), \tag{2.30}$$

$$h_x(\mathbf{p, q}) = \frac{1}{8I_{xx}} (\mathbf{p}^T \cdot \{-q_1, q_0, q_3, -q_2\})^2, \tag{2.31}$$

17

$$h_y(\mathbf{p}, \mathbf{q}) = \frac{1}{8I_{yy}}(\mathbf{p}^T \cdot \{-q_2, -q_3, q_0, q_1\})^2, \tag{2.32}$$

$$h_z(\mathbf{p}, \mathbf{q}) = \frac{1}{8I_{zz}}(\mathbf{p}^T \cdot \{-q_3, q_2, -q_1, q_0\})^2, \tag{2.33}$$

The symplectic integration can be done by applying the Trotter theorem on equations. 2.31,

2.32 and 2.33. Unlike the Velocity-Verlet algorithm mentioned above, the NO-SQUISH

integrator has to be decomposited into up to 10 terms.

3.0   SIMULATION RESULTS

3.1   COMPUTATIONAL DETAILS

The molecular dynamics code used for the simulations was written by myself and is named HOMURA. The DPP model[14] provides the force field for the neutral water cluster; while the OEPM model implemented in the PISCES code,[24] developed in the Jordan group, is used for describing the interaction of the excess electron with the water cluster. The OEPM model[14,24] closely reproduces the electron binding energies from ab-*initio* calculations. Since the DPP model employs rigid water monomers, the NO-SQUISH integrator[39] is combined for doing the molecular dynamics simulations. In this report, the water hexamer anion observed was chosen to test the code. This system was selected for study as it is the best characterized $(H_2O)_n^-$ cluster, both experimentally and computationally.[22,41] Three structures, tweezers, AA (double H-bond acceptors), and book (Figure. 2), were used as the starting structure. The book isomer of the neutral cluster is of particular interest as the Johnson
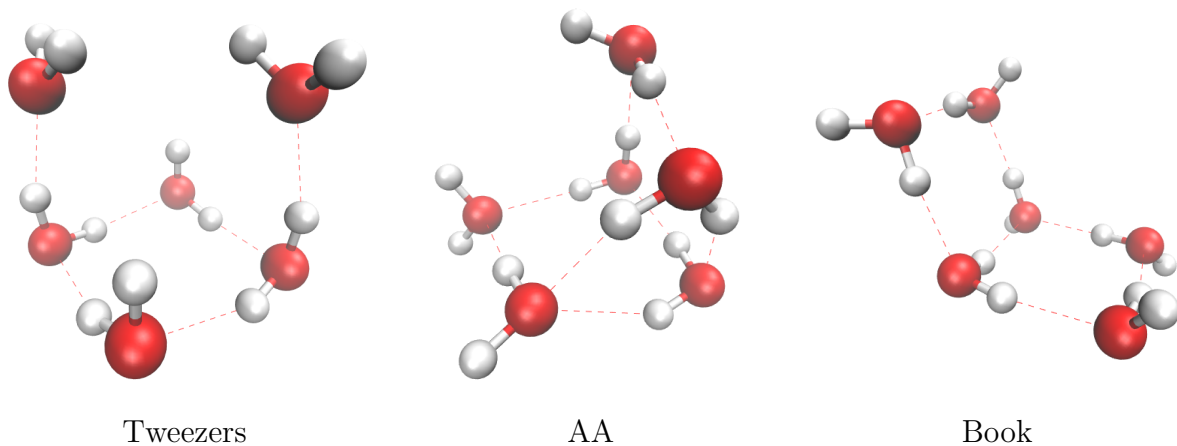
Tweezers   AA   Book

Figure 2: Initial structures of $(H_2O)_6^-$ used in the simulations.

group has established that it is the precursor of the dominant (AA) form of the anion in the experiments.[42] The initial velocities of molecules in the cluster were randomly assigned based on Maxwell-Boltzmann distributions at temperatures of 50, 100 and 150K; center-of-mass translation and cluster rotation were not removed as they did not affect the properties interested. NVE simulations were carried out with a time step of 0.001 picosecond.

3.2   RESULTS

The time dependence of the dipole of the neutral water cluster is shown in Figure 2, and the VDE of the excess electron obtained from simulations starting from the tweezers, AA and book structures are reported in Figures 3, 4 and 5. From the figures, it is seen that the

electron binding energy (EBE) loosely tracks the dipole (Figure. 6, 7, and 8), as expected for dipole-bound anions. The wavefunctions at time 2.0 picoseconds are shown in Figure 10.

In the simulations starting from the tweezers structure, rearrangement to the more stable AA structure occurs within 200 femtoseconds, even at temperatures as low as 50K. In the T= 100 and 150K simulations, the cluster rearranges to a low-dipole non-AA structure around 1.8 picoseconds.[42] In the simulations starting from the AA structure, the basic structural motif is preserved for the duration of the simulations, i.e., up to $\sim$ 5 picoseconds. However there are fluctuations where the dipole moment drops about 1 Debye with a corresponding decrease in the EBE.[43] In the simulations starting from the book structure, rearrangement to a prism structure is observed in the T=50 and 100K simulations. Surprisingly, the book structure is kept in the T=150K simulations. Although the book to AA rearrangement is seen experimentally,[42] in none of the simulations starting from the book structure was transformation to the AA structure was observed. This is apparently due to the high rearrangement barrier, which has been calculated to be 17.6 kJ/mol.[44] The evolution of the dipole moment and EBE for the simulations starting with the three different initial structures at initial temperature = 50K are reported in Figure 11.
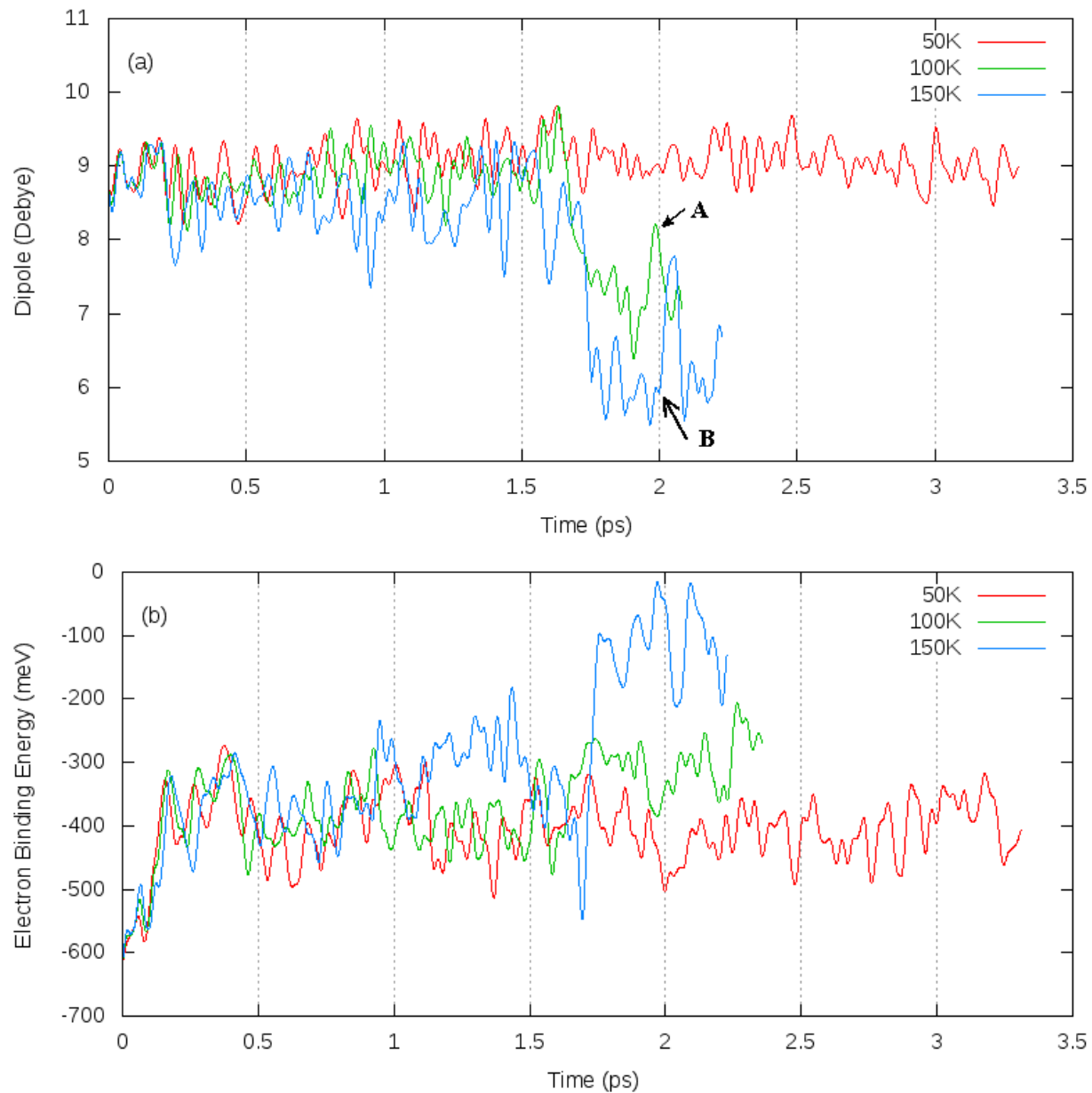
Figure 3:

Time evolution of (a) the dipole moment and (b) electron binding energy of $(H_2O)_6^-$ in simulations starting from the tweezers structure. The structures at 2 picoseconds at T=100 and 150K, noted as **A** and **B** are shown in Figure 10.

Figure 4:

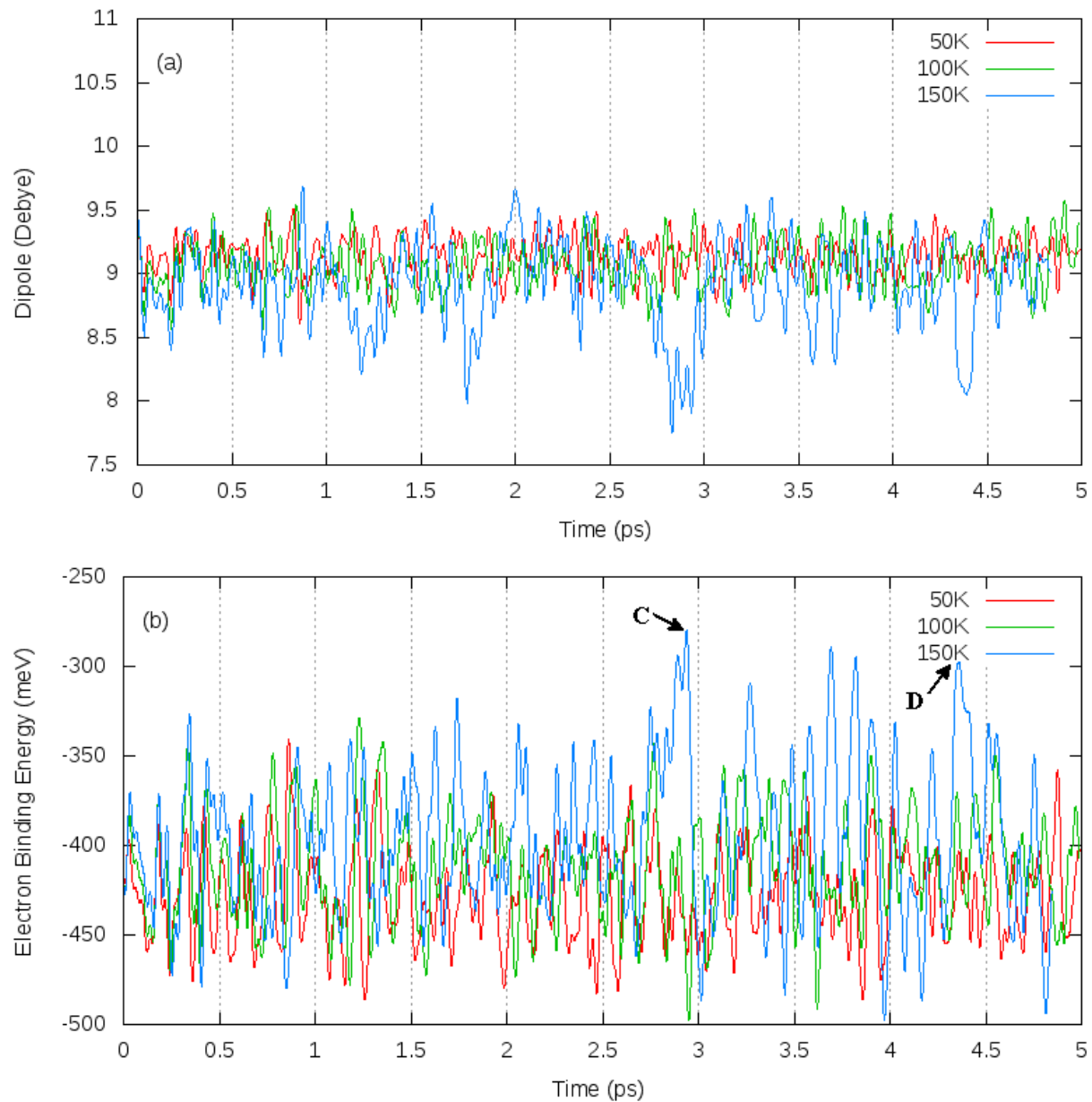Time evolution of (a) the dipole moment and (b) electron binding energy of $(H_2O)_6^-$ in simulations starting from the AA structure. The structures at two specified time points, **C** and **D**, for the simulation with initial temperature 150K are shown in Figure 9.
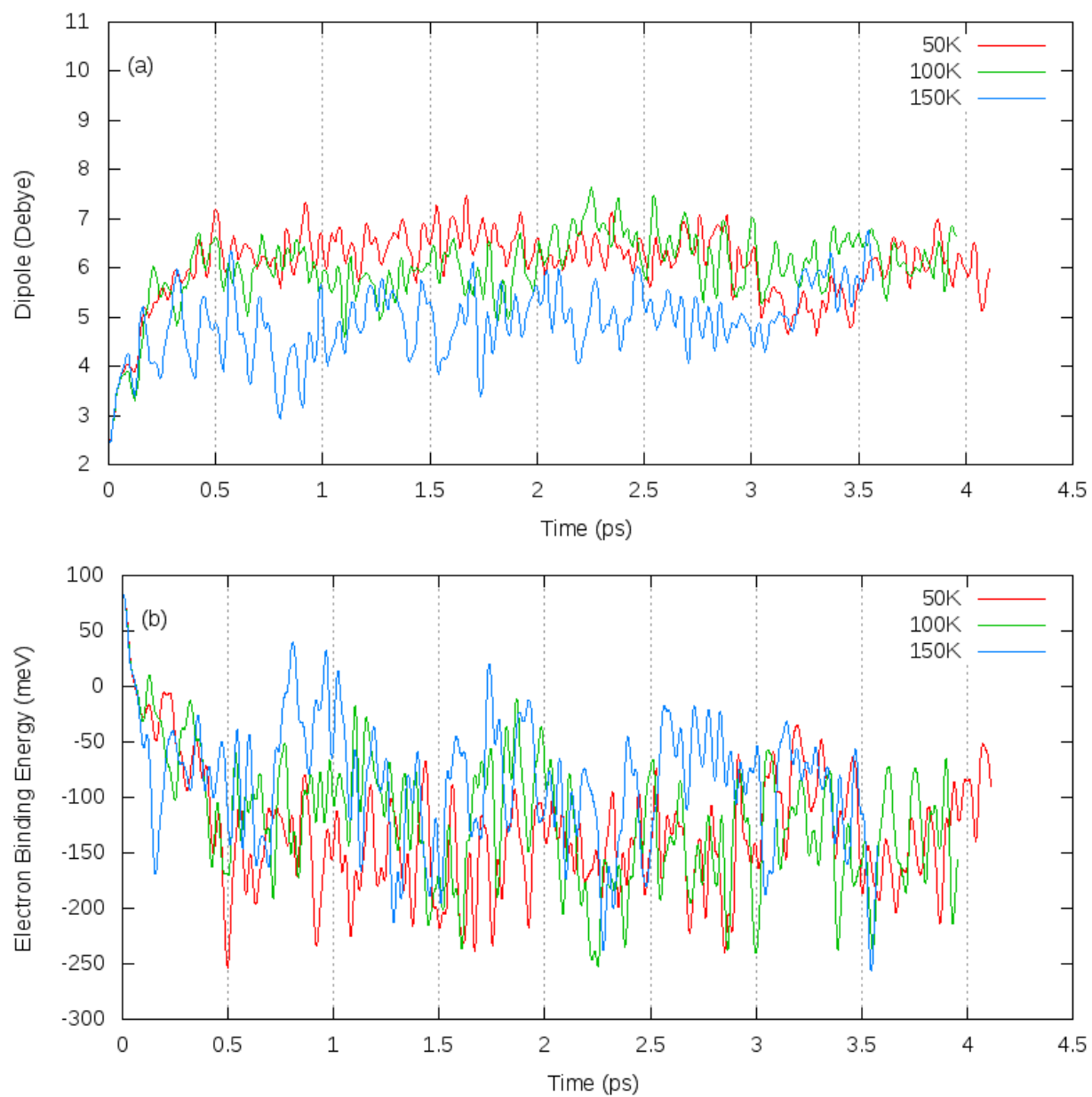
Figure 5: Time evolution of (a) the dipole moment and (b) electron binding energy of $(H_2O)_6^-$ in simulations starting from the book structure.
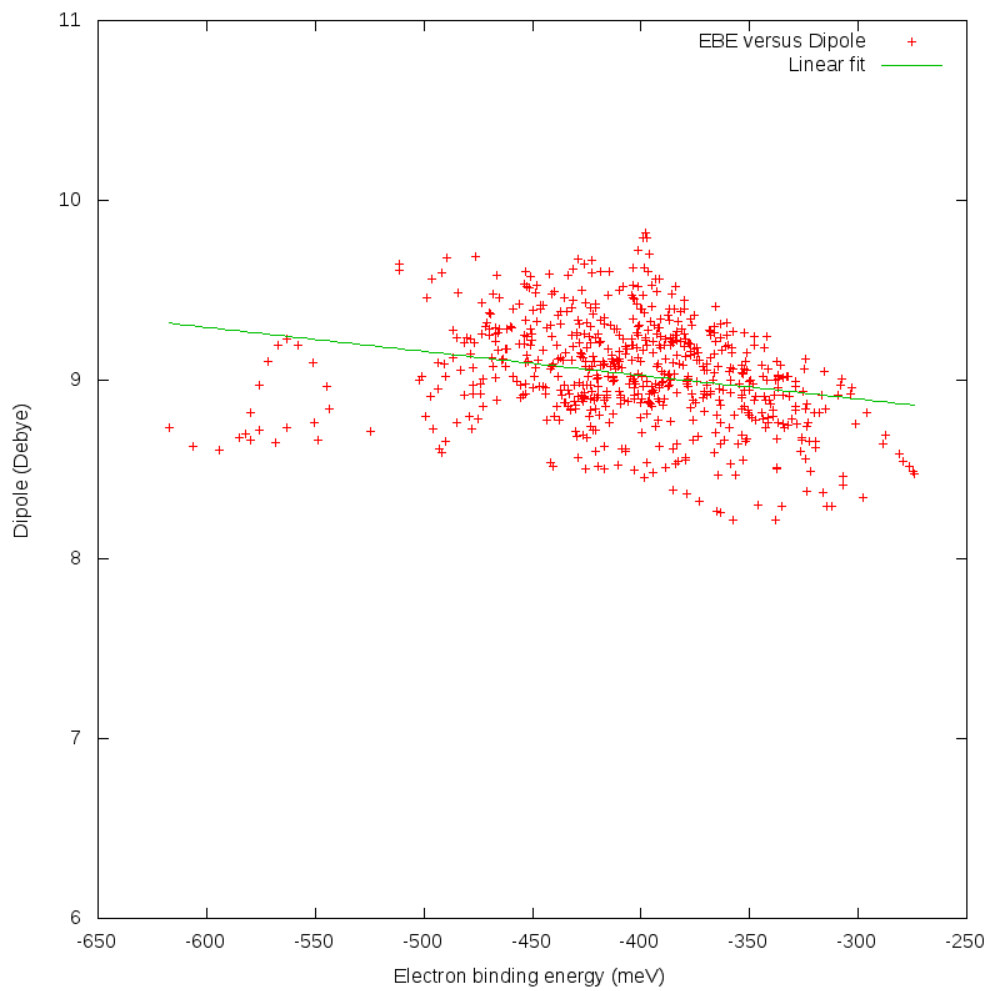
Figure 6:

Relationship between the electron binding energy and the dipole moment of the neutral cluster from a simulation starting from the tweezers structure.

Figure 7:

Relationship between the electron binding energy and the dipole moment of the neutral cluster from a simulation starting from the AA structure.
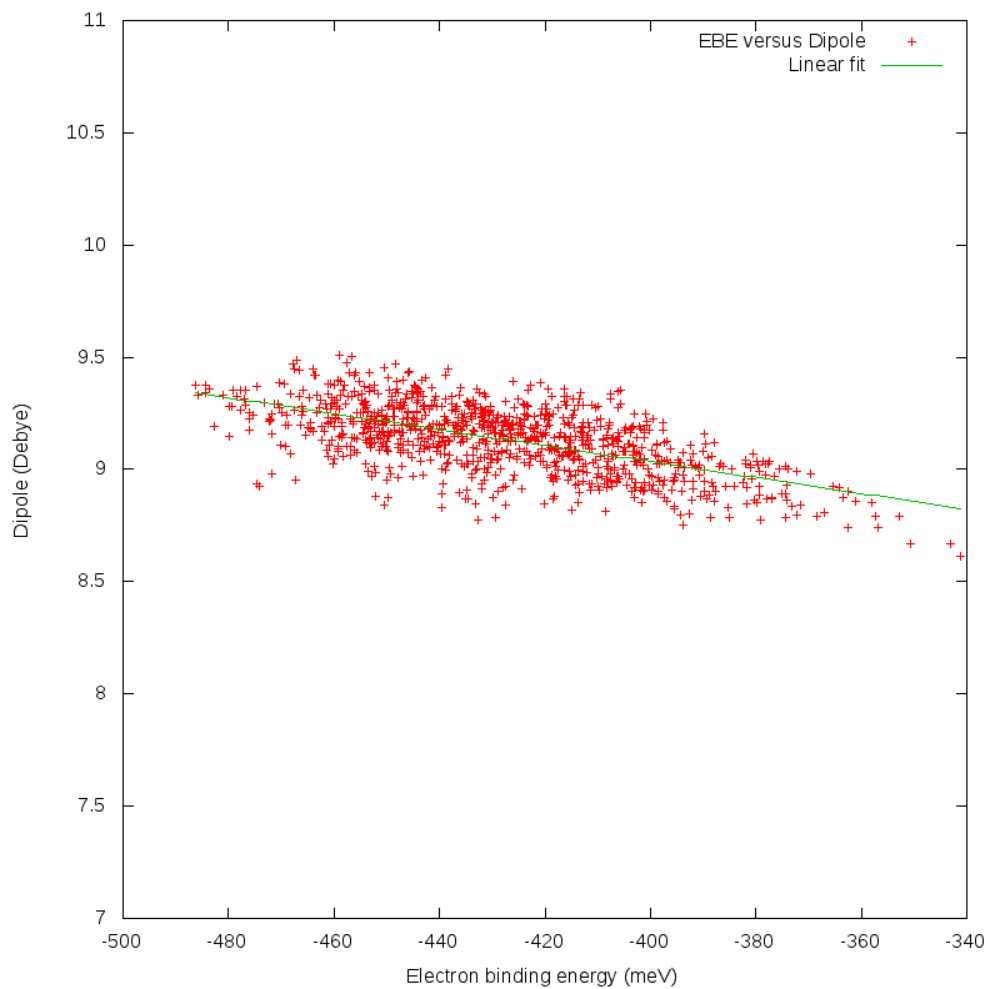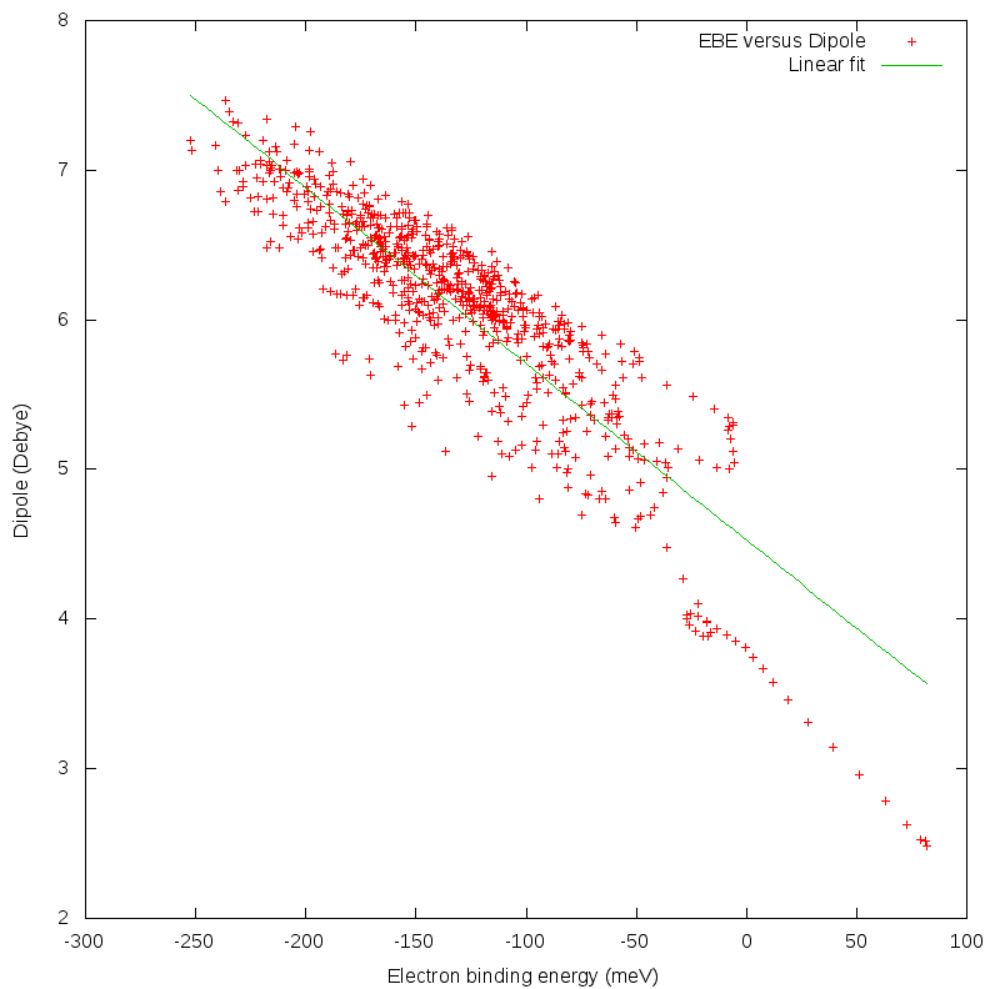
Figure 8:

Relationship between the electron binding energy and the dipole moment of the neutral cluster from a simulation starting from the book structure.
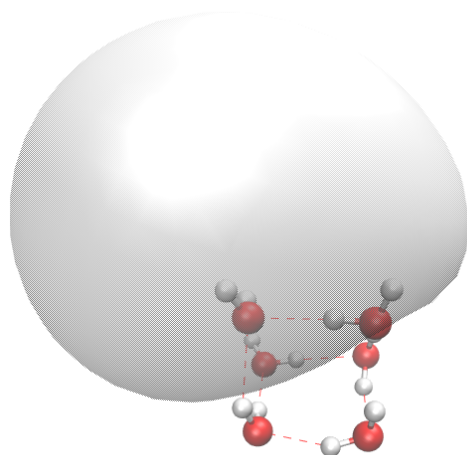
C at time t=2.94 ps, Dipole = 7.99 Debyes, EBE = −280 meV
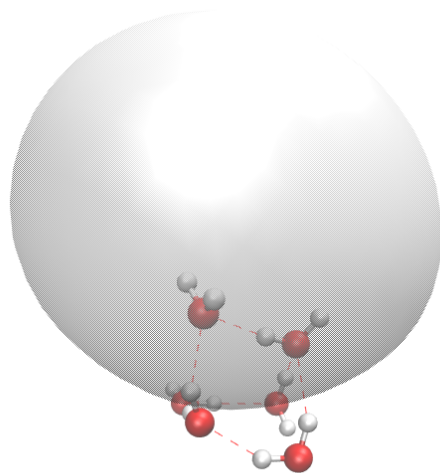
D at time t=4.35 ps, Dipole = 8.17 Debyes, EBE = −300 meV

Figure 9:

Structures **C** and **D** sampled in the T=150K simulation of $(H_2O)_6^-$ starting from the AA structure. The isosurface of excess electron wavefunction is drawn with an absolute value of $0.01e^{1/2} \cdot \text{Bohr}^{-3/2}$.

Tweezers   AA   Book

(1) Initial temperature: 50K

(2) Initial temperature: 100K

(3) Initial temperature: 150K
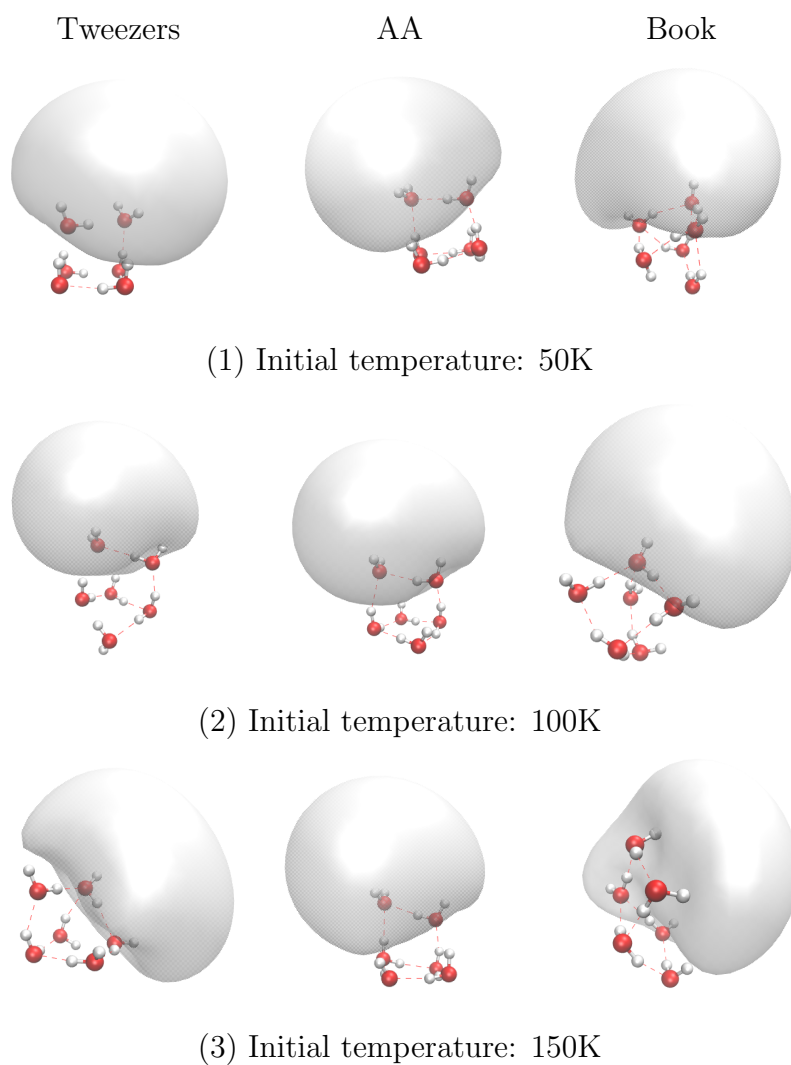
Figure 10:

Wavefunction of the excess electron at 2.0 ps, isosurface drawn with an absolute value of $0.01\mathrm{e}^{1/2} \cdot \mathrm{Bohr}^{-3/2}$. Structures **A** and **B** in Figure 3 are shown as the leftmost pictures in the second and the third row.
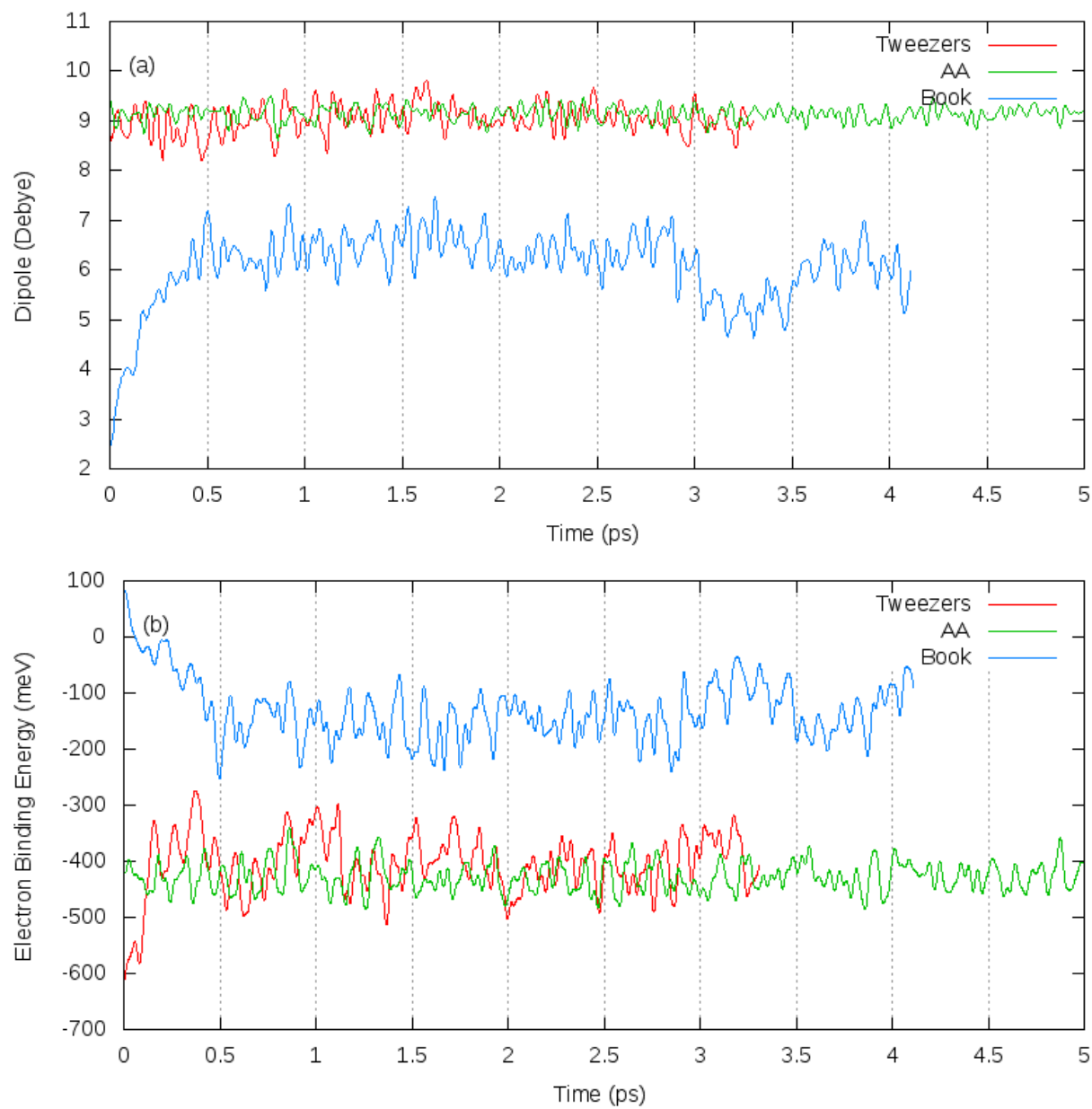
Figure 11:

Comparison of time evolution of (a) the dipole moment and (b) electron binding energy of $(H_2O)_6^-$ in simulations starting from three structures, with initial temperature T=50K.

4.0 FUTURE WORK

In the future one important direction is to map out the pathways for conversion of the surface- to cavity-bound excess electron states of $(H_2O)_n^-$ clusters.[17] An initial challenge is to model the book to AA rearrangement of $(H_2O)_6^-$, which is evidenced by experiments[42]. At present the MD simulation requires several days on a single CPU core to acquire ~ 5 picoseconds of simulation time for $(H_2O)_6^-$. Times much longer than that are required to overcome the barrier in the potential energy surface. Although parts of the OEPM code have been parallelized, there is still a bottleneck at matrix diagonalization step. By use of parallel sparse matrix eigensolvers it should be possible to achieve a speedup of $10 \sim 20 \times$ of the code depending on the system size. In addition, it is likely that the rate of isomerization would be greatly enhanced upon inclusion of nuclear quantum effects, e.g., by mean of path-integral molecular dynamics (see below). This has been found to be the case for neutral water clusters.[45–47] It is also a goal to use molecular dynamics simulations to simulate vibrational energy redistribution following vibrational excitation of a specific OH stretch mode in a

$(H_2O)_n^-$ cluster. This will require making the force field flexible. One possible approach would be introducing intramolecular terms for O-H bonds and H-O-H angle similar to AMOEBA force field,[48] another possibility could be fitting the potential curve of one water molecule using B-splines. A refitting of the OEPM parameters might also be necessary. The flexible force field can then be used to theoretically predict the vibrational spectra. Since many experimental studies have used vibrational spectroscopy[6,49] on $(H_2O)_n^-$, being able to predict spectra for different isomers would be very valuable.

The excess electron in bulk water is also of interest. Periodic boundary conditions (PBC) are needed for such simulations. Here the key quantity to calculate is the electronic absorption spectrum.[50] To reduce the computational cost of such calculations, we will explore various approximations for describing the long range electron-water interactions.[11]

Due to the light mass of the hydrogen nucleus, vibrational quantum effects, in particular, zero-point motion, are expected to be important in the $(H_2O)_n^-$ clusters. Quantum delocalization and tunneling are also expected to be significant.[47] To date all Monte-Carlo and MD simulations of $(H_2O)_n^-$ clusters have ignored nuclear quantum effects. Path integral molecular dynamics (PIMD) would be able to address these quantum effects.[51,52]

Finally, a long-term goal is coupling our one-electron models with traditional electronic structure methods to treat systems such as $(H_2O)_n^-(CO_2)$. This problem has been studied

experimentally by the Johnson group.[53] Here the CO_2 would be treated all-electron and the

water molecules by means of our model potential approach. This would facilitate simulation

of the reduction of CO_2 into industrial useful materials, e.g. HCOOH, CH_2O or CH_3OH.[54,55]

BIBLIOGRAPHY

[1] J. Boag and E. Hart, "Absorption spectra in irradiated water and some solutions," *Nature*, vol. 197, no. 4862, p. 45, 1963.

[2] B. Garrett, D. Dixon, and et al., "Role of water in electron-initiated processes and radical chemistry: issues and scientific advances," *Chemical Review*, vol. 105, p. 355, 2005.

[3] J. Coe, G. Lee, J. Eaton, S. Arnoid, H. Sarkas, K. Bowen, C. Ludewigt, H. Haberland, and D. Worsnop, "Photoelectron spectroscopy of hydrated electron cluster anions, $(H_2O)^-_{n=2\sim69}$," *The Journal of Chemical Physics*, vol. 92, no. 6, p. 3980, 1990.

[4] N. Hammer, J. Roscioli, and M. Johnson, "Identification of two distinct electron binding motifs in the anionic water clusters: a vibrational spectroscopic study of the $(H_2O)^-_6$ isomers," *The Journal of Physical Chemistry A*, vol. 109, p. 7896, 2005.

[5] J. Verlet, A. Bragg, A. Kammrath, O. Cheshnovsky, and D. Neumark, "Comment on 'characterization of the excess electrons in water-cluster anions by quantum simulations'," *Science*, vol. 310, p. 1769b, 2005.

[6] D. Neumark, "Spectroscopy and dynamics of excess electrons in clusters," *Molecular Physics*, vol. 106, p. 2183, 2008.

[7] A. Khan, "Ab initio studies on $(H_2O)_{14}^-$ clusters: existence of surface and interior-bound extra electrons," *The Journal of Chemical Physics*, vol. 125, p. 024307, 2006.

[8] A. Madarász, P. Rossky, and L. Turi, "Interior- and surface- bound excess electron states in large water cluster anions," *Science*, vol. 130, p. 124319, 2009.

[9] O. Marsalek, F. Uhlig, J. van de Vondele, and P. Jungwirth, "Structure, dynamics, and reactivity of hydrated electrons by ab initio molecular dynamics," *Accounts of Chemical Research*, vol. 45, no. 1, p. 23, 2012.

[10] O. Marsalek, F. Uhlig, and P. Jungwirth, "Electrons in cold water clusters: An ab initio molecular dynamics study of localization and metastable states," *The Journal of Physical Chemistry C*, vol. 114, no. 48, p. 20489, 2010.

[11] F. Uhlig, O. Marsalek, and P. Jungwirth, "Electron at the Surface of Water: Dehydrated or Not?," *The Journal of Physical Chemistry Letters*, vol. 4, no. 2, p. 338, 2013.

[12] O. Marsalek, F. Uhlig, T. Frigato, B. Schmidt, and P. Jungwirth, "Dynamics of electron localization in warm versus cold water clusters," *Physical Review Letters*, vol. 105, no. 4, p. 043002, 2010.

[13] F. Uhlig, O. Marsalek, and P. Jungwirth, "Unraveling the complex nature of the hydrated electron," *The Journal of Physical Chemistry Letters*, vol. 3, no. 20, p. 3071, 2012.

[14] A. Defusco, D. P. Schofield, and K. D. Jordan, "Comparison of models with distributed polarizable sites for describing water clusters," *Molecular Physics*, vol. 105, no. 19-22, p. 2681, 2007.

[15] L. Turi and D. Borgis, "Analytical investigations of an electron-water molecule pseu-

dopotential. ii. development of a new pair potential and molecular dynamics simulations," *The Journal of Chemical Physics*, vol. 117, p. 6186, 2002.

[16] L. Turi, W. Sheu, and P. Rossky, "Characterization of excess electorns in water-cluster anions by quantum simulations," *Science*, vol. 309, p. 914, 2005.

[17] L. Turi, A.Madarász, and P. Rossky, "Excess electron localization sites in neutral water clusters," *The Journal of Chemical Physics*, vol. 125, p. 014308, 2006.

[18] B. Thole, "Molecular polarizabilities calculated with a modified dipole interaction," *Chemical Physics*, vol. 59, p. 341, 1981.

[19] K. Tang and J. Toennies, "An improved simple model for the van der waals potential based on universal damping functions for the dispersion coefficients," *The Journal of Chemical Physics*, vol. 80, p. 3726, 1984.

[20] C. Burnham and S. Xantheas, "Dvelopment of transferable interaction models for water. III. reparameterization of an all-atom polarizable rigid model (TTM2-R) from first principles," *The Journal of Chemical Physics*, vol. 116, p. 1500, 2002.

[21] T. Dunning, "Gaussian basis sets for use in correlated molecular calculations. I. The atoms boron through neon and hydrogen," *The Journal of Chemical Physics*, vol. 54, p. 724, 1989.

[22] T. H. Choi, T. Sommerfeld, S. L. Yilmaz, and K. D. Jordan, "Discrete variable representation implementation of the One-Electron Polarization Model," *Journal of Chemical Theory and Computation*, vol. 6, no. 8, p. 2388, 2010.

[23] T. Choi and K. Jordan, "Analytical graient for geometry optimizations of $(H_2O)_n^-$ clusters as described by the pm1 polarzable model," *Chemical Physics Letters*, vol. 464, p. 139, 2008.

[24] V. K. Voora, J. Ding, T. Sommerfeld, and K. D. Jordan, "A self-consistent polarization potential model for describing excess electrons interacting with water clusters," *The Journal of Physical Chemistry. B*, vol. 117, p. 4365, 2013.

[25] J. Light, I. Hamilton, and J. Lill, "Generalized discrete variable approximation in quantum mechanics," *Journal of Chemical Physics*, vol. 82, p. 1400, 1985.

[26] R. Littlejohn, M. Cargo, T. Carrington, K. Mitchell, and B. Poirier, "Investigations of multidimensional discrete variable representation basis sets," *Journal of Chemical Physics*, vol. 116, p. 8691, 2002.

[27] D. Baye and P. Heenen, "Generalised meshes for quantum mechanical problems," *Journal of Physics A: Mathematial and General*, vol. 19, p. 2041, 1986.

[28] R. Littlejohn and M. Cargo, "Multidimensional discrete variable representation bases: Sinc functions and group theory," *Journal of Chemical Physics*, vol. 116, p. 7350, 2002.

[29] M. Cargo and R. Littlejohn, "Tetrahedrally invariant discrete variable representation basis on the sphere," *Journal of Chemical Physics*, vol. 117, p. 27, 2002.

[30] L. Landau and E. Lifshitz, *Mechanics*. Butterworh-Heinemann, 3 ed., 1976.

[31] L. Landau and E. Lifshitz, *Statistical Mechanics, Part I*. Butterworh-Heinemann, 3 ed., 1976.

[32] M. Tuckerman, *Statistical Mechanics: Theory and Molecular Simulation*. Oxford Universitt Press, 2010.

[33] H. Trotter, "On the product of semi-groups of operators," *Proceedings of the American Mathematical Society*, vol. 10, p. 545, 1951.

[34] W. Swope, H. Andersen, P. Berens, and K. Wilson, "A computer simulation method for the calculation of equilibrium constants for the formation of physical clusters of

molecules: Application to small water clusters," *The Journal of Chemical Physics*, vol. 76, p. 648, 1982.

[35] K. Feng and M. Qin, *Symplectic geometric Algorithms for Hamiltonian systems.* Springer, 2010.

[36] D. Beeman, "Some multistep methods for use in molecular dynamics calculations," *Journal of Computational Physics*, vol. 20, p. 130, 1976.

[37] H. Anderson, "Rattle: A "velocity" version of the shake algorithm for molecular dynamics calculations," *Journal of Computational Physics*, vol. 52, p. 24, 1983.

[38] B. Leimkuhler and R. Skeel, "Symplectic numerical integrators in constrained hamiltonian systems," *Journal of Computatonal Physics*, vol. 112, p. 117, 1994.

[39] T. F. Miller, M. Eleftheriou, P. Pattnaik, A. Ndirango, D. Newns, and G. J. Martyna, "Symplectic quaternion scheme for biophysical molecular dynamics," *The Journal of Chemical Physics*, vol. 116, no. 20, p. 8649, 2002.

[40] H.Goldstein, *Classical Mechanics.* Addison-Wesley, 1980.

[41] C. Pérez, M. T. Muckle, D. P. Zaleski, N. A. Seifert, B. Temelso, G. C. Shields, Z. Kisiel, and B. H. Pate, "Structures of cage, prism, and book isomers of water hexamer from broadband rotational spectroscopy.," *Science*, vol. 336, no. 6083, p. 897, 2012.

[42] E. Diken, W. Robertson, and M. Johnson, "The vibrational spectrum of the neutral $(H_2O)_6$ precursor to the "magic" $(H_2O)_6^-$ cluster anion by Argon-mediated, population-modulated electron attach spectroscopy," *The Journal of Physical Chemistry A*, vol. 108, p. 64, 2004.

[43] J. Roscioli, N. Hammer, and M. Johnson, "Infrared spectroscopy of water cluster anions, $(H_2O)_{n=3-24}^-$ in the HOH bending region: persistence of the double H-Bond acceptor

(AA) water molecule in the excess electron binding site of the class I isomers," *The Journal of Physical Chemistry A*, vol. 110, p. 7517, 2006.

[44] T. Choi and K. Jordan, "Potential energy landscape of the $(H_2O)_6^-$ cluster," *Chemical Physics Letter*, vol. 475, p. 293, 2009.

[45] M. Tuckerman, D. Marx, M. Klein, and M. Parrinello, "On the quantum nature of the shared proton in hydrogen bonds," *Science*, vol. 275, p. 817, 1997.

[46] C. Swalina, Q. Wang, A. Chakraborty, and S. Hammes-Schiffer, "Analysis of nuclear quantum effects on hydrogen bonding," *The Journal of Physical Chemistry A*, vol. 111, p. 2206, 2007.

[47] X. Li, B. Walker, and A. Michaeldes, "Quantum nature of the hydrogen bond," *Proceeding of National Academy of Sciences*, vol. 108, p. 6369, 2011.

[48] J. W. Ponder, C. Wu, P. Ren, V. S. Pande, J. D. Chodera, M. J. Schnieders, I. Haque, D. L. Mobley, D. S. Lambrecht, R. A. DiStasio, M. Head-Gordon, G. N. I. Clark, M. E. Johnson, and T. Head-Gordon, "Current status of the AMOEBA polarizable force field," *The Journal of Physical Chemistry B*, vol. 114, no. 8, pp. 2549–2564, 2010.

[49] N. Hammer, J. Shin, J. Headrick, E. Diken, J. Roscioli, G. Weddle, and M. Johnson, "How do small water clusters bind an excess electron," *Science*, vol. 306, p. 675, 2004.

[50] J. Casey, R. Larsen, and B. Schwartz, "Resonance Raman and temperature-dependent electronic absorption spectra of cavity and noncavity models of they hydrated electron," *Proceeding of National Academy of Sciences*, vol. 110, p. 2712, 2013.

[51] D. Marx and M. Parrinello, "Ab-*initio* path integral molecular dynamics," *Z. Phys. B Condens. Matter*, vol. 95, p. 143, 1994.

[52] M. Tuckerman, D. Marx, M. Klein, and M. Parrinello, "Efficient and general algorithms

for path integral car-parrinello molecular dynamics," *The Journal of Chemical Physics*, vol. 104, p. 5579, 1996.

[53] K. Breen, A. DeBlase, T. Guasco, V. Voora, K. Jordan, T. Nagata, and M. Johnson, "Bottom-up view of water network-mediated CO_2 reduction using cryogenic cluster ion spectroscopy and direct dynamics simulations," *The Journal of Physical Chemistry A*, vol. 116, p. 903, 2012.

[54] F. Huang, G. Lu, L. Zhao, H. Li, and Z. Wang, "The catalytic role of n-heterocyclic carbene in a metal-free conversion of carbon dioxide into methanol: A computational mechanism study," *Journal of American Chemical Society*, vol. 132, p. 12388, 2010.

[55] T. Arai, S. Sato, K. Uemura, T. Morikawa, T. Kajino, and T. Motohiro, "Photoelectrochemical reduction of CO_2 in water under visible-light irradiation by a p-type inp photocathode modified with an electropolymerized ruthenium complex," *Chemical Communications*, vol. 46, p. 6944, 2010.

PUBLICATIONS

1. H. K. Geraldi, C. M. Levaitt, A. F. DeBlase, M. A. Johnson, A. B. McCoy, X. Su, and K. D. Jordan, Structural Characterization of Electron-Induced Proton Transfer in the Formic Acid Dimer Anion $(HCOOH)_2^-$ with Vibrational and Photoelectron Spectroscopies, *The Journal of Chemical Physics*, vol. 136, p. 134318, 2012.

2. H. Gerardi, A. DeBlase, X. Su, K. D. Jordan, A. B. McCoy, and M. A. Johnson, Unraveling the Anomalous Solvatochromic Response of the Formate Ion Vibrational Spectrum: An Infrared, Ar-tagging Study of the HCO_2^-, DCO_2^-, and HCO_2^--H_2O Ions, *The Journal of Physical Chemistry Letters*, vol. 2, p. 2437, 2011.

3. C. Lu, X. Su and P. E. Floreancig, Stereocontrolled Cyanohydrin Ether Synthesis through Chiral Brønsted Acid-Mediated Vinyl Ether Hydrocyanation, *The Journal of Organic Chemistry*, vol. 78, p. 9366, 2013

4. Z. D. Pozun, X. Su, and K. D. Jordan, Establishing the Ground State of the Disjoint Diradical Tetramethyleneethane with Quantum Monte Carlo, *Journal of the American Chemical Society*, vol. 135, p. 13862, 2013